



Baseline

How does the tidal cycle influence the estuarine dynamics of microplastics?

Ravena Santiago Alves^a, Victória Maria Carneiro dos Santos^a, Rebeca Amon Moreira^a, Gabriel Chrystian Lima de Alcantara^a, Emanuelle Ribeiro Lima^a, Bárbara Pereira Paiva^a, Carlos Eduardo Peres Teixeira^a, Vasco Stascxak Neto^b, Alejandro Pedro Ayala^b, David Chelazzi^c, Johnny Peter Macedo Feitosa^d, Marcelo Oliveira Soares^a, Tommaso Giarrizzo^a, Michael Barbosa Viana^{a,*}

^a Instituto de Ciências do Mar (LABOMAR), Universidade Federal do Ceará (UFC), Fortaleza, Brazil

^b Departamento de Física, Universidade Federal do Ceará (UFC), Fortaleza, Brazil

^c Department of Chemistry "Ugo Schiff" and CSGI, University of Florence, Florence, Italy

^d Departamento de Química, Universidade Federal do Ceará (UFC), Fortaleza, Brazil

ARTICLE INFO

Keywords

Microplastic
Plastic debris
Tidal fluctuation
River-sea transport
Low-inflow estuary

ABSTRACT

Estuaries are the main pathway for the microplastics (MPs) to enter into the oceans. However, factors that drive river-sea transport of MPs are not yet fully understood. Therefore, our research investigated the influence of the tidal cycle on the abundance and characteristics of MPs in an urban estuary, through high-frequency sampling (every 2–3 h) using a plankton net (120 µm mesh size) in two seasons (rainy and dry seasons). The results showed that the abundance of MPs decreased during the ebb tide and increased during the flood tide. A positive correlation was found between MP abundance and water height in both seasons. The shapes and colors of MPs varied significantly throughout the tidal cycle. The results show that tides are key agents in the transfer of MPs and cannot be neglected in models of the global contribution of plastic pollution from rivers to oceans.

Microplastics (MPs) are emerging pollutants that have been the subject of recent studies due to their ubiquity, ability to transport other persistent pollutants, and the negative effects they can have on ecosystem functioning, such as obstruction of the gastrointestinal tract of small organisms and biomagnification (Elizalde-Velázquez and Gómez-Oliván, 2021). Estuaries are important pathways of MPs transport into the marine environment, but have complex dynamics of flow exchanges between the river and the sea, mainly driven by tidal cycles and seasonal variations in river discharge (Malli et al., 2022). Most studies investigating the occurrence of MPs in estuaries conducted spatial sampling without considering tidal conditions (Hossain et al., 2023; Rajan et al., 2023). However, it is known that MP concentrations can vary by a factor of 1000 within a tidal cycle (Cohen et al., 2019). Therefore, high-frequency temporal sampling is strongly recommended for estuaries under the influence of tides (Defontaine and Jalón-Rojas, 2023).

Only recently the influence of the tidal cycle on the transport of fluvial MPs has been addressed with studies focusing on Asian (China, Thailand, and Indonesia) and European (England and France) large estuaries (Chinfak et al., 2021; Diansyah et al., 2024; Pasquier et al., 2024; Stead et al., 2020; Wei et al., 2023). To date, there have been no studies in South American short estuaries assessing the abundance and composition of MPs in the water over a tidal cycle.

Low-inflow estuaries are common worldwide, but their study is usually neglected (Largier, 2023). These shallow ecosystems are extremely sensitive to anthropogenic stresses and climate change (Soares et al., 2021). Due to the long estuarine residence time, caused by the low river runoff, these short estuaries tend to retain contaminants during the dry season (Moura and Lacerda, 2022). On the other hand, during the rainy season, the increase in river runoff leads to the discharge of contaminants into the sea, including MPs (Lima et al., 2015). However, estuarine dynamics are complex, and the factors that

* Corresponding author.

E-mail addresses: ravenasantiago@alu.ufc.br (R.S. Alves), victoriamariaa@alu.ufc.br (V.M.C. dos Santos), rebecaamon@alu.ufc.br (R.A. Moreira), gabriel.chrystian@alu.ufc.br (G.C.L. de Alcantara), emanuellemima@alu.ufc.br (E.R. Lima), barbara@ufc.br (B.P. Paiva), carlos.teixeira@ufc.br (C.E.P. Teixeira), vasconeto@fisica.ufc.br (V.S. Neto), ayala@fisica.ufc.br (A.P. Ayala), david.chelazzi@unifi.it (D. Chelazzi), johnnyquimico@gmail.com (J.P.M. Feitosa), marcelosoares@ufc.br (M.O. Soares), tgiarrizzo@gmail.com (T. Giarrizzo), vianamb@ufc.br (M.B. Viana).

<https://doi.org/10.1016/j.marpolbul.2024.117471>

Received 16 September 2024; Received in revised form 14 December 2024; Accepted 15 December 2024

Available online 19 December 2024

0025-326X/© 2024 Elsevier Ltd. All rights are reserved, including those for text and data mining, AI training, and similar technologies.

drive river-sea transport of MPs are not yet fully understood. Therefore, the objectives of this baseline assessment were (1) to assess the effects of tidal cycles on the abundance and morphological characteristics of MPs in two seasons (rainy and dry seasons), and (2) to determine the polymer composition of MPs in an urban low-inflow estuary.

The Cocó River is an urban river with extensive mangrove forest areas that flows through the Brazilian capital with the highest population density in the country and is exposed to multiple anthropogenic pressures (Ward et al., 2023), which are even more severe upstream. The Cocó River is located in the semi-arid region of Ceará state. It is a shallow hydrographic basin of about 50 km in length and 485 km² in total area (SEMACE, 2010). The catchment area covers a large part of the city of Fortaleza, the fourth most populous city in the country with over 2.4 million inhabitants. The average accumulated rainfall in the rainy season (February to May) is 1137.9 mm, while in the dry season (August to November), it is only 52.9 mm (INMET, 2020).

The flow rate of the river was estimated at 6 m³/s during the rainy season and 3 m³/s during the dry season (Molisani et al., 2006). The estuary is shallow with an average depth of 2 m and is dominated by semi-diurnal mesotides with average amplitudes ranging from 1 m during neap tides to 3 m during spring tides (Pereira et al., 2015). All estuaries on the Ceará coast are saline or hypersaline during the dry season and may have residual transport landward at this time. However, the Cocó estuary receives freshwater influx throughout the year due to illegal sewage dump and also due to the flow of freshwater from wastewater treatment plants into the estuary (Freitas et al., 2016).

Sampling was carried out in the middle of the river channel at the deepest point (7 m) close to the estuary entrance (3°46'53.6"S 38°26'13.9"W) (Fig. 1). The water sampling was conducted every 2–3 h, three during ebb tide and three during flood tide, resulting in a total of six samples per tidal cycle. Sampling took place during the rainy season (May 30, 2022) and the dry season (October 25, 2022) at spring tides. Surface water samples were collected from the top 15 cm of the water column using a plankton net (120 µm; 0.3 m Ø; 1 m) positioned on the

side of the boat and kept floating against the water flow for 1 min at an average speed of 2 knots. A mechanical flow meter (Model, 2030R, General Oceanic) was installed in the opening of the net to measure the volume of filtered water. After the trawl, the outside of the net was rinsed with river water that had been pre-filtered through a 63 µm stainless steel sieve, and the cod end was rinsed with pre-filtered distilled water. The samples were then transferred to glass bottles and stored at −20 °C until further analysis in the laboratory.

To collect hydrodynamic data, an Acoustic Doppler Current Profiler (ADCP) was anchored at the sampling site to record the water level over a period of 13-h during the sampling days. In addition, depth, temperature and salinity vertical profiles were measured at intervals of 10 to 30 min using a CastAway CTD probe.

The analysis procedures were based on the methodology described by Gago et al. (2018). After thawing, the water samples were filtered using stainless steel sieves with a mesh size of 5 mm and 63 µm to remove large debris and concentrate the collected sample. The concentrated samples on the sieve were then transferred to beakers and rinsed with distilled water pre-filtered. A 10 % potassium hydroxide solution at a ratio of 1:3 (v/v) was then added to the samples to promote digestion of the organic matter in an oven at 40 °C for 72 h. Due to the large amount of debris and particulate matter suspended in the samples, the MPs were separated by density difference using a zinc chloride solution with a density of 1.6 g/cm³ added to the samples at a ratio of 1:3 (v/v) and left to rest for 24 h in separatory funnels. After this time, the supernatant was filtered through a glass fiber filter with a mesh size of 0.7 µm (GF-1, 47 mm Ø, Macherey-Nagel) using a vacuum pump. Finally, the filters were placed in glass Petri dishes and dried for 24 h at room temperature (25 °C) in a desiccator for later observation.

The filters were carefully inspected using a Leica S8 APO stereomicroscope (maximum magnification of 80×) equipped with a high-resolution Leica EC3 digital camera. The MP particles were measured and photographed using the Leica Application Suite software (LAS EZ Version 3.4.0/2016). The MPs were classified by shape into fibers,

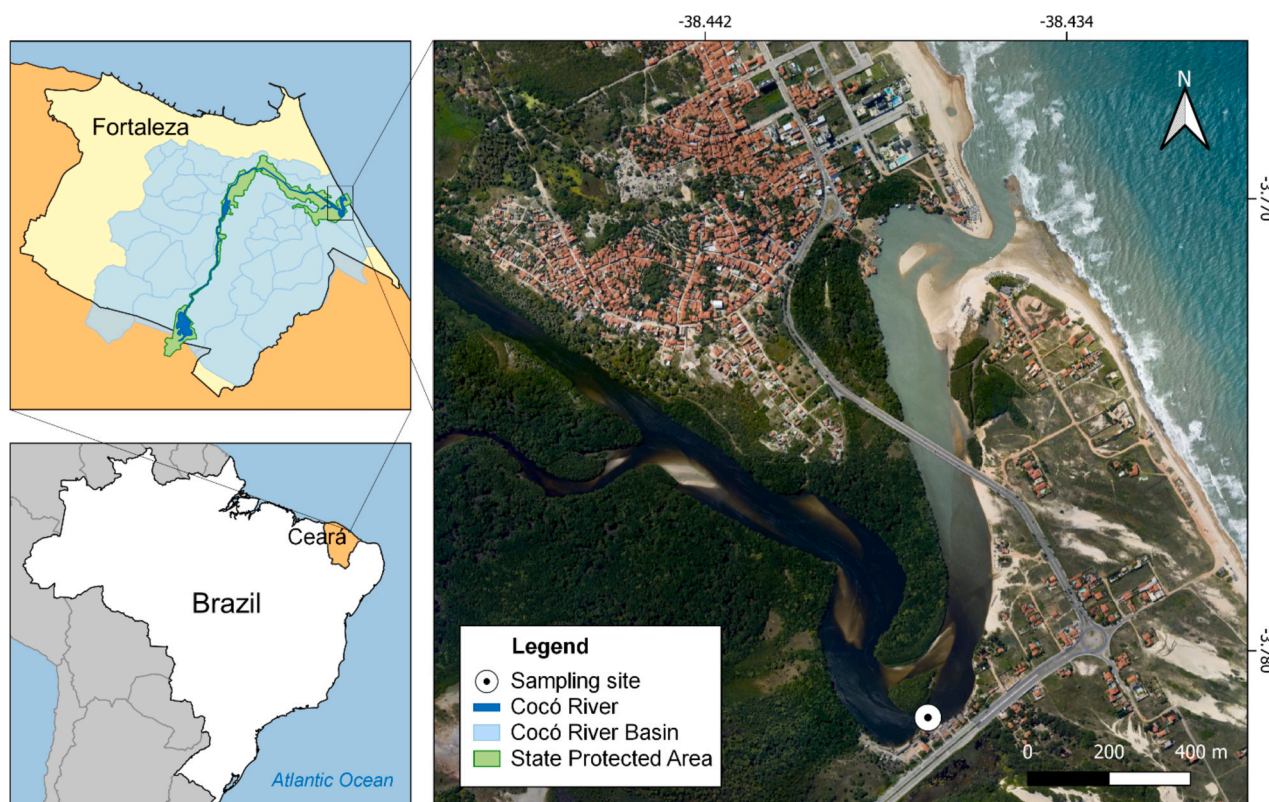


Fig. 1. High-frequency sampling site over tidal cycle in the Cocó River estuary (Fortaleza, Brazil).

fragments, films, rubbers, foams, and microbeads, and by color into blue, black (including gray), white, transparent, red (including pink and orange), green, yellow, and others (including purple, brown, and multicolored). The MPs were categorized into five size classes: 0.12–0.3 mm; 0.3–0.5 mm; 0.5–1 mm; 1–2 mm; and 1–5 mm (Gago et al., 2018).

The polymer composition of 30 MP particles was analyzed by Raman spectroscopy and Fourier transform infrared spectroscopy (FTIR). The polymer composition of particles smaller than 500 μm was analyzed by Raman spectroscopy and that of particles larger than 500 μm by Fourier transform infrared spectroscopy (FTIR) (Jayalakshamma et al., 2023). The Raman spectra were obtained using a Horiba LabRam HR spectrometer, equipped with a charge-coupled device (CCD) detector and a 600 grooves/mm diffraction grating. A 785 nm solid-state laser was used for excitation. The spectra were identified by comparison with reference spectra found in the literature (Jin et al., 2022; Prabakaran et al., 2002; Ren et al., 2023). The FTIR spectra were obtained using an IRPrestige-21 FTIR spectrometer (SHIMADZU – Tokyo, Japan). The samples were dispersed in potassium bromide (KBr) crystals and analyzed in a spectral range from 4000 to 400 cm^{-1} , resolution 4 cm^{-1} and 64 scans. The FTIR spectra were compared with reference spectra found in the literature (De Frond et al., 2021; Kroon et al., 2018; Xu et al., 2019).

To reduce the possibility of contamination by synthetic fibers, cotton lab coats and nitrile gloves were used during sample processing in a fume hood. All containers and instruments used were made of glass or stainless steel. All solutions used were pre-filtered through glass fiber filters (0.7 μm pore size), including distilled water. All surfaces were cleaned with 70 % ethanol and the experimental apparatus were

immersed in an acidic solution (1 % HNO_3), rinsed three times with filtered distilled water before use and covered with aluminum foil. To check for air contamination, a glass fiber filter was left open in a Petri dish next to the work area. In addition, a control blank was run for each batch analysis and analyzed in the same way as the samples. The particles present in the blank controls were counted and classified according to shape, color, and size class. The contamination found in the blank controls was used to correct the amount of MPs found in the samples. For this purpose, the particles from the blank controls with similar characteristics to those in the samples were subtracted from the total amount (Munno et al., 2023) (Table S1).

The statistical analysis and data visualization were performed using Microsoft Office Excel, PRIMER v7 (Clarke and Gorley, 2015) and JASP (Version 0.18.1). Pearson correlation was conducted to assess the association between i) the abundance of MPs particles and water height, and ii) the abundance of MPs particles and particle size classes. Whenever a significant correlation was identified, linear regression analysis was conducted to develop an equation predicting the relationship between the response and independent variables.

A permutational multivariate analysis of variance (PERMANOVA) was performed to test for differences in total abundance of MPs, particle characteristics by shape, color, and size classes between the seasons (i.e., rainy and dry season), and tidal stage (i.e., ebb and flood tide) (Anderson, 2008). Statistical significance was tested using 9999 permutations of the residuals with a reduced model (Freedman and Lane, 1983) and the Type III (partial) sums of squares (Anderson, 2008). The PERMANOVA was performed on a Bray-Curtis similarity matrix,

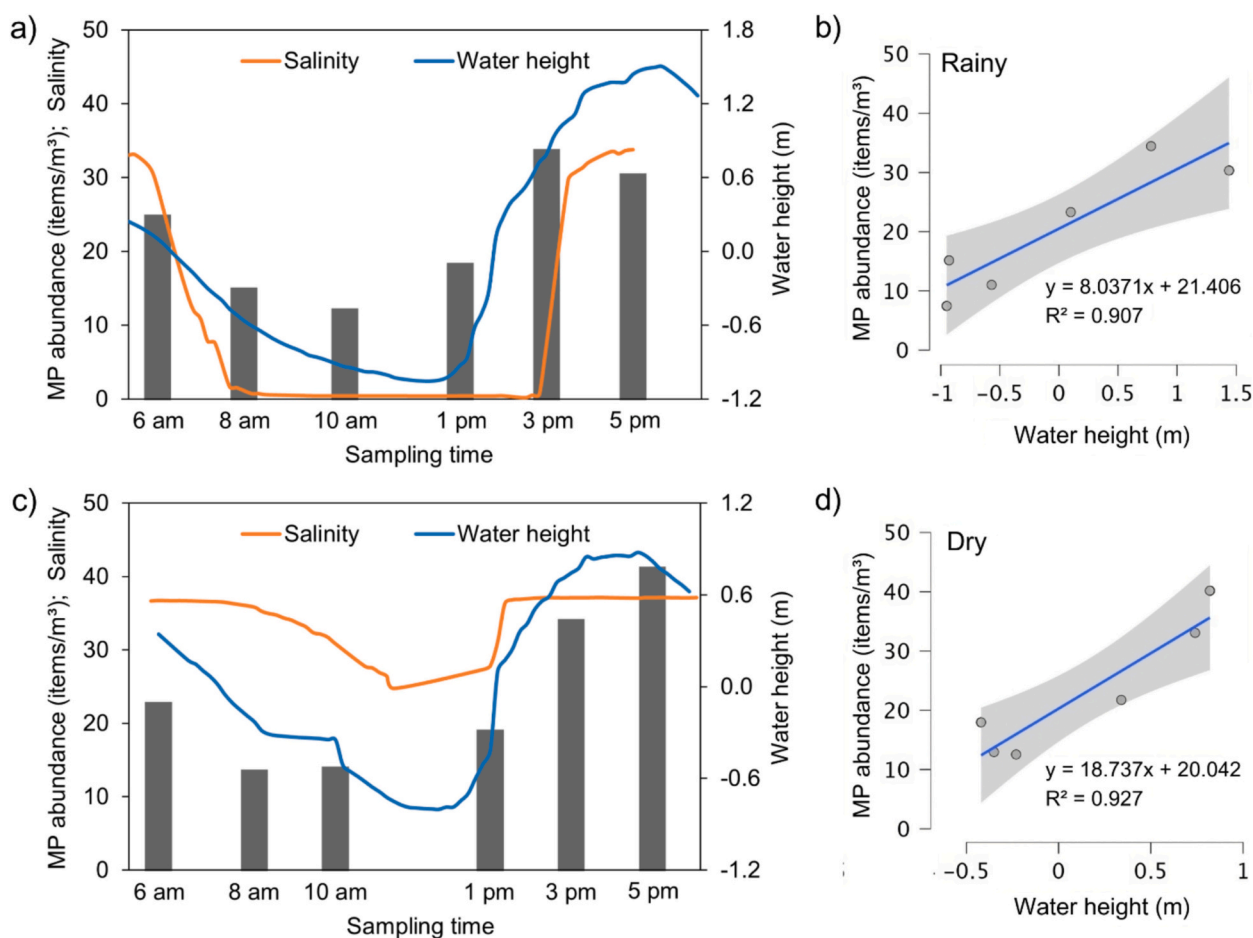


Fig. 2. (a, c) Abundance of microplastics in surface water through a tidal cycle and (b, d) scatter plots showing the corresponding regression lines and regression equations between the dependent variable y (microplastic abundance) and the independent variable x (water height) in the Cocó River estuary (Fortaleza, Brazil). Shaded area indicates 95 % confidence interval for the linear regression.

calculated from the fourth root transformed abundance data.

A total of 5307 MPs were detected in the surface water samples. The abundance of MPs during the tidal cycle ranged from 10.96 to 32.55 items/m³ in the rainy season, and from 12.37 to 40.00 items/m³ in the dry season (Fig. 2a–c). Significant differences in the MP abundance were detected between the tidal stages (PERMANOVA, Pseudo-F = 6.965, $p = 0.037$), whereas seasons and interactions tidal stage \times season had no significant differences. The mean abundance of MPs during flood tide (28.27 ± 9.08 items/m³) was almost 2 times higher than during ebb tide (15.85 ± 5.34 items/m³). A positive correlation was found between MP abundance and water height in both seasons (Rainy season: $R^2 = 0.907$, $p = 0.013$; Dry season: $R^2 = 0.927$, $p = 0.008$) (Fig. 2b–c). These findings highlight the importance of considering tidal timing to ensure representative sampling of MPs, with the resulting regression equations (Fig. 2b–c) being a crucial tool for accurately estimating MP abundance at different tidal times (Li et al., 2023).

The abundance of MPs showed a clear pattern in relation to the tides in both seasons, gradually decreasing along the ebb tide and rapidly increasing during flood tide. Similar results were found in the Dong River, China, where the abundance of MPs ranged from 11.15 at low tide to 95.26 items/m³ at high tide, and was strongly related to the water level and tidal flow direction (Li et al., 2023). Other studies have also reported a higher abundance of MPs during flood tide compared to ebb tide (Oo et al., 2021; Stead et al., 2020; Wei et al., 2023). In contrast, recent studies have found opposite results for different estuaries, which they generally attribute to the dilution of MP concentration due to the

inflow of seawater during the flood tide (Diansyah et al., 2024; Wu et al., 2024; Chinfak et al., 2021; Tang-Siri et al., 2024). Therefore, it is important to consider various local hydrological factors that may influence the variation of MP abundance during tidal fluctuations, such as mixing, residence time, seasonal variation on river discharge, tidal asymmetry, and the specific geometry of estuaries (Biltcliff-Ward et al., 2022).

In the study area, the MPs transported by the low-inflow estuary discharge during the ebb tide may be deposited in the bottom or partially trapped in the mangrove forests, and not completely transported to the ocean (Liu et al., 2022). In addition, due to the shallow depth and low riverine discharge during most of the year when there is no rainwater input, sandbars usually form along the lower estuary at low tide and the mouth of the estuary eventually becomes partially closed due to the accumulation of sediments (Fig. S1a) (Largier, 2023), which may serve as traps for the interception of MPs that are more susceptible to deposition in low-energy environments (Harris, 2020).

The water level rise and rapid change in flow direction during faster flood currents in the shallow estuary (Fig. S1b) may resuspend MPs into the water column (Govender et al., 2020), which are then transported upstream and carried back downstream during the ebb tide of the next tidal cycle (Wu et al., 2022). This short and low-inflow estuary may have a high capacity for MP accumulation due to the prolonged residence time caused by absence of river discharge (Cardoso-Mohedano et al., 2023), which occurs mainly during the dry season when saltier water is prevalent (tidal average salinity = 34.7 ± 3.5) (Fig. 2c).

Table 1

Comparison of the abundance of microplastics in mesotidal estuaries worldwide. The ranges of the abundance in a tidal cycle and/or the mean abundance in different tidal stages (ebb and flood tide) are shown.

| Location | Sample type | Sampling method | | Abundance (items/m ³) | Reference |
|-------------------------------------|------------------|---|-------------|--|-----------------------------|
| | | Device | Mesh size | | |
| Cocó River Estuary, Brazil | Surface water | Plankton net | 120 μ m | Range: 10.96–32.55 (rainy) Range: 12.37–40.00 (dry) Mean: 15.85 ± 5.34 (ebb tide) Mean: 28.27 ± 9.08 (flood tide) | This study |
| Musi River Estuary, Indonesia | Surface water | Steel bucket (100 L) | 25 μ m | Mean: 622.22 (ebb tide) Mean: 298.89 (flood tide) | (Diansyah et al., 2024) |
| Yangtze River, China | Surface water | Manta net | 330 μ m | Mean: 2.44 ± 1.30 (ebb tide) Mean: 1.48 ± 2.07 (flood tide) | (Wu et al., 2024) |
| Yangtze River, China | Water column | Submerged stainless-steel pumps (100 L) | 330 μ m | Range: 15.6–121.1 (wet) Range: 28.9–218.9 (dry) Mean: 41.1 ± 18.9 (ebb tide) Mean: 72.8 ± 42.1 (flood tide) | (Wei et al., 2023) |
| Dong River, China | Subsurface water | Plankton net | 64 μ m | Range: 11.15–95.26 Mean: 53.46 ± 29.63 | (Li et al., 2023) |
| Jiulong River Estuary, China | Surface water | Stainless-steel bucket (105 L) | 45 μ m | Range: 312.4–1106.1 Mean: 782.5 ± 201.5 | (Wu et al., 2022) |
| Tapi-Phumduang River, Thailand | Subsurface water | Bulk (5 L) | 5 μ m | Range: 320–1680 Mean: 1370 ± 220 (low tide) Mean: 500 ± 90 (high tide) | (Chinfak et al., 2021) |
| Chao Phraya River Estuary, Thailand | Water column | Stainless-steel bucket and Van Dorn bottle (6 L–10 L) | 16 μ m | Range: 440–16,930 Mean: 4030 ± 4230 (ebb tide) Mean: 6250 ± 4470 (low tide) Mean: 3440 ± 3340 (flood tide) Mean: 2060 ± 1540 (high tide) | (Tang-Siri et al., 2024) |
| Chao Phraya River Estuary, Thailand | Surface water | Manta net | 335 μ m | Mean: 3.11 (ebb tide) Mean: 5.16 (flood tide) | (Oo et al., 2021) |
| Chao Phraya River Estuary, Thailand | Surface water | Neuston net | 330 μ m | Range: 0.17–0.59 (spring tide) Mean: 0.35 ± 0.16 (spring tide) | (Sukhsangchan et al., 2020) |

The abundance of MPs in the low-inflow estuary was compared with that of other mesotidal estuaries worldwide at different tidal stages (Table 1). The mean abundance of MPs in the Cocó River estuary (22.06 ± 9.62 items/m³) was about half than in the Dong River estuary, China (53.46 ± 29.63 items/m³) (Li et al., 2023). This could be related to greater local contamination in the Dong estuary but also to the smaller mesh size of the plankton net used (64 μ m), which catches smaller MPs (Zheng et al., 2021). In contrast, Wei et al. (2023) found a higher mean abundance of MPs in the Yangtze River estuary, China (83.95 ± 19.5 items/m³) by sampling with a submerged pump with a larger mesh size than in the present study (330 μ m), while studies using a trawl method with the same mesh size reported much lower abundance of MPs (0.33 to 2.48 items/m³) (Wu et al., 2024). The use of distinct sampling methods also resulted in considerable differences in MP abundance in the Chao Phraya River estuary, Thailand.

The abundances of MPs in the study area were lower than in studies using bulk sampling or stainless-steel bucket collections (Table 1). The trawl method used in this study collects a larger volume of water compared to the bulk sampling method, which could be a key factor in the variation in MP abundance, as small-volume grab samples can measure up to 10⁴ items/L higher abundances than net samples, even when sampled simultaneously (Watkins et al., 2021). This highlights the influence of sampling methods on MP abundance, making comparisons between estuaries difficult.

The predominant shapes were fibers (50 %), films (25 %), rubbers (13 %), and fragments (11 %), while foams and microbeads together accounted for 1 % of the total MPs found in surface water (Figs. S2, 3a). MPs shape distribution exhibited significant variation throughout the tidal cycle (Pseudo-F = 4.853, $p = 0.004$), with fibers, films, and rubbers consistently dominating in both ebb and flood tides (Fig. 3b–c). However, their abundance was notably higher during flood tide, suggesting that tidal influx may preferentially transport and accumulate these MPs. The fibers are derived from the domestic and industrial laundering process of textiles, and released into the aquatic environment mainly through the discharge of Wastewater Treatment Plants (WWTP) (Acharya et al., 2021). In Fortaleza, 37.2 % of the population is not connected to the sewage system (SNIS, 2022). Therefore, untreated wastewater discharged directly into the river and clandestine sewage connections in the urban drainage network can be an important pathway for the diffusion of MPs (Vasconcelos et al., 2021).

Fragments and films can originate, for example, from the

degradation of plastic bottles, plastic bags and food packaging (Osman et al., 2023). These MPs may have entered the aquatic environment through the leaching of waste in landfills or even by littering in the river or on streets (He et al., 2019). Exposure of these solid wastes to the weather and intense solar radiation in the region causes the drying out of plastics, which accelerates the wear and fragmentation process of MPs (Sorasan et al., 2022). The rubber particles result from the wear and tear of tyres on roads and enter aquatic environments mainly through stormwater runoff and atmospheric deposition (Kole et al., 2017). The high levels of rubber in the studied estuary may be associated with the proximity of bridges, heavily trafficked roads, and boat landing sites (Leads and Weinstein, 2019).

The MPs found were almost evenly distributed across all size classes and were predominant in the size class of 0.5–1 mm (29 %), followed by 0.12–0.30 mm (23 %), 0.3–0.5 mm (20 %), 1–2 mm (20 %), and 2–5 mm (8 %) (Fig. 4a). No significant differences in size classes of MPs were detected throughout the tidal cycle (Pseudo-F = 1.926, $p = 0.178$) (Fig. 4b–c). Particles smaller than 1 mm accounted for 72 % of the total MPs found in the Cocó River estuary, similar to the findings of Praved et al. (2024), who reported that particles <1 mm accounted for >72 % of the MPs in the surface water of the Cochin estuary, India. Similar results were found in Guanabara Bay, Brazil (Olivatto et al., 2019), the Chao Phraya River, Thailand (Oo et al., 2021), and the estuaries of Shanghai, China (Zhang et al., 2019).

The predominance of small-sized MPs is due to the rapid progressive fragmentation of plastic debris in the environment (Banik et al., 2024). The size of MPs influences their bioavailability to aquatic organisms, as smaller particles are more likely to be ingested by lower trophic level organisms such as phytoplankton and zooplankton (Wright et al., 2013). Moreover, the smaller the size of the MPs, the greater their specific surface area (surface area/volume), and consequently the greater their potential to adsorb pollutants (Cunningham et al., 2022).

The predominant colors of MPs were transparent (32 %), white (22 %), black (21 %), and blue (15 %), while red (3 %), green (3 %), yellow (3 %), and others (2 %) were the smallest fractions (Fig. 5a). The colors of MPs varied significantly throughout the tidal cycle (Pseudo-F = 2.407, $p = 0.037$) (Fig. 5b–c). The high proportions of transparent and white MPs were mainly due to the amount of fibers and films of these colors (78 % and 71 %, respectively), whereas black MPs were mainly represented by rubbers (61 %) (Fig. S3). In the Pearl River estuary, China, transparent and white colors accounted for 73.8 % of the MPs

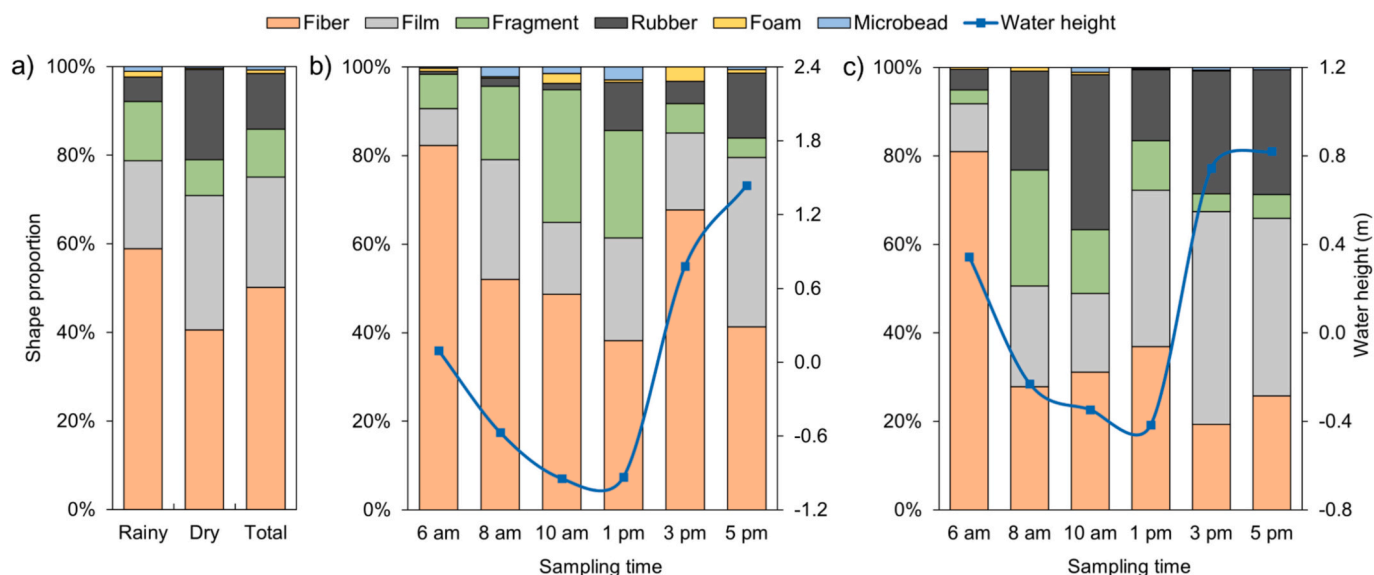


Fig. 3. Shape proportion of microplastics in surface water during the rainy and dry seasons (a), and through a tidal cycle in the rainy season (b) and dry season (c) in the Cocó River estuary (Fortaleza, Brazil).

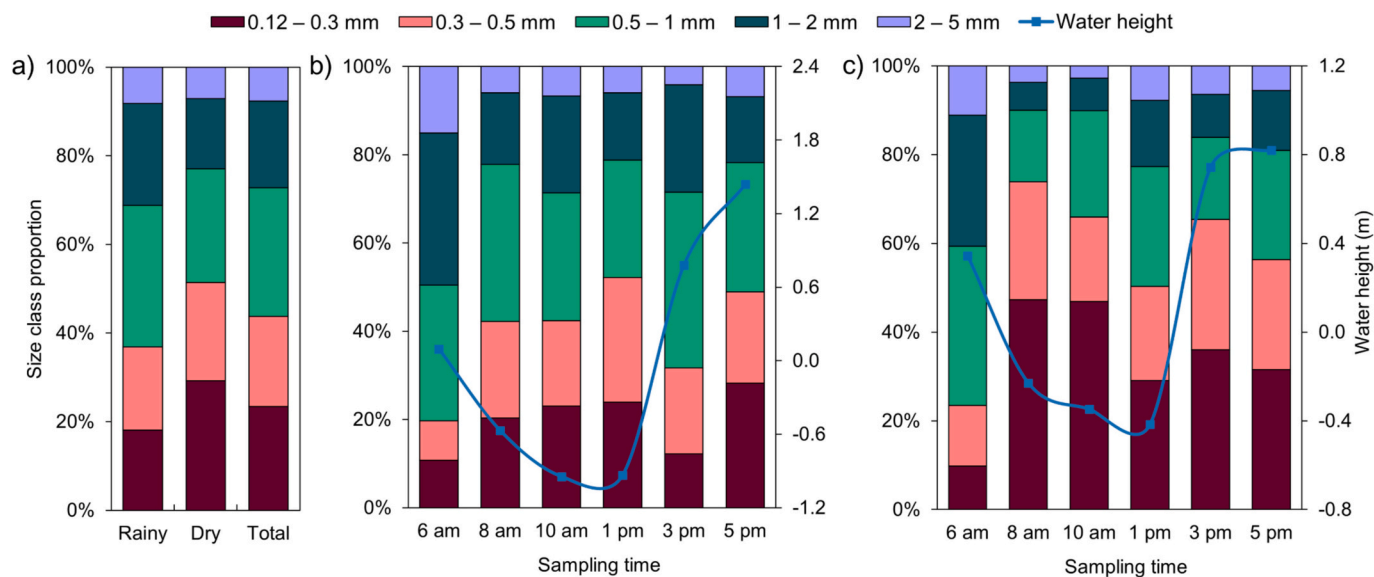


Fig. 4. Size class proportion of microplastics in surface water during the rainy and dry seasons (a), and through a tidal cycle in the rainy season (b) and dry season (c) in the Cocó River estuary (Fortaleza, Brazil).

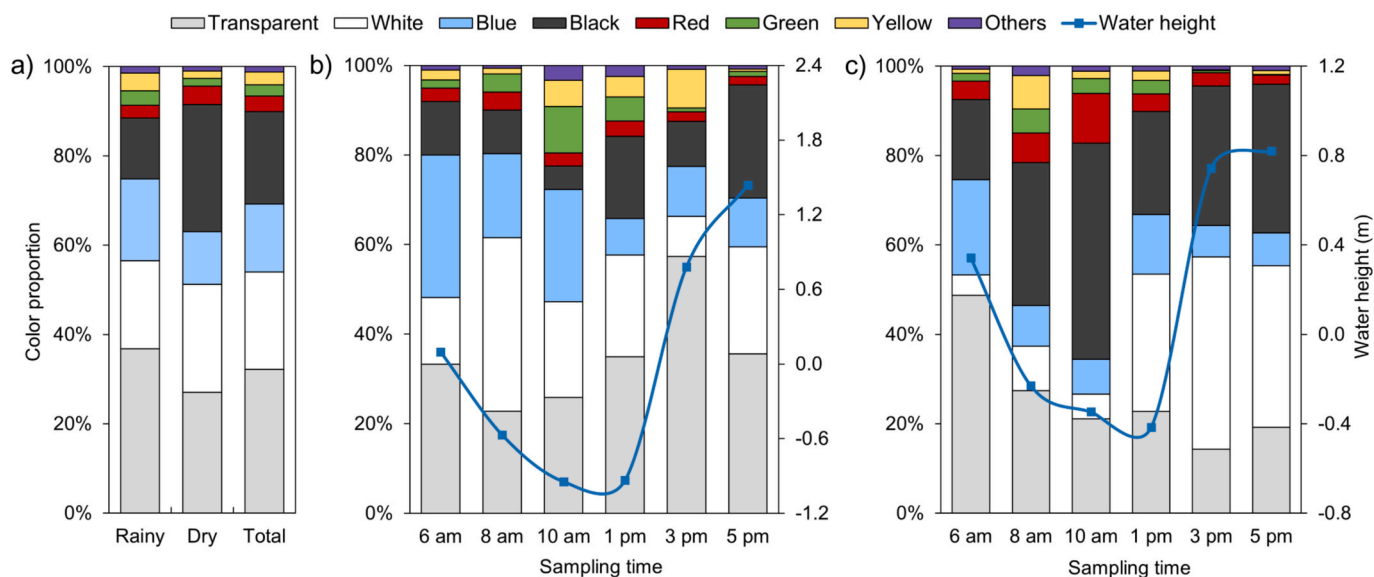


Fig. 5. Color proportion of microplastics in surface water during the rainy and dry seasons (a), and through a tidal cycle in the rainy season (b) and dry season (c) in the Cocó River estuary (Fortaleza, Brazil). (For interpretation of the references to color in this figure legend, the reader is referred to the web version of this article.)

found in the water, and about one-third (33.1 %) of the transparent MPs were films (Lam et al., 2020). Studies in the Yellow River estuary, China, showed that the majority of fibers were transparent or white (Han et al., 2020). The higher abundance of transparent MPs in the Cocó River estuary may be partly explained by color fading due to the exposure time of the MPs to UV light and other atmospheric agents (Wong et al., 2020).

The predominant type of polymer was polyethylene (PE, 44 %), followed by polystyrene (PS, 13 %), natural rubber (10 %), latex (10 %), polyethylene-polypropylene copolymer (PE-PP, 7 %), polyethylene terephthalate (PET, 5 %), polypropylene (PP, 3 %), polyvinyl chloride (PVC, 3 %), and indigo blue dye (3 %) (Fig. 6). The occurrence of low-density polymers, such as PE, PS, and PP, was expected as they float on the water surface and are predominant in the coastal environment (Hidalgo-Ruz et al., 2012). These are the polymers most produced by the global plastics industry and are commonly used in the manufacture of plastic bags, bottles, food packaging, and foams (Wang et al., 2019).

Natural rubber may derive from tire wear particles, which are composed of a complex mixture of elastomers (Kole et al., 2017). Latex is commonly used in coating materials, paints, adhesives, and sealants (Tangsongcharoen and Paulis, 2024). The presence of high-density polymers in surface water, such as PET and PVC, may indicate the resuspension of MPs due to intense mixing of the water column (Diez-Pérez et al., 2023). PVC is mainly used in the construction industry, while PET may originate from the disposal of fishing gear such as ropes and trawl nets (Devereux et al., 2023; Lin et al., 2020). Anthropogenic fibers with indigo blue dye may originate from the laundering of synthetic fabrics and are mainly released into the aquatic environment through the discharge of wastewater into rivers (Giarratano et al., 2022).

In conclusion, this baseline assessment investigated the influence of the tidal cycle and seasonal variations on the dynamics of MPs in an urban low-inflow estuary. The abundance of MPs in surface water

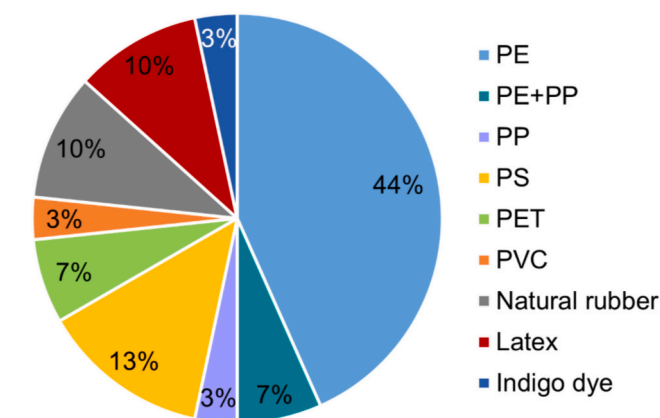


Fig. 6. Types of polymers found in the surface water of the Cocó River estuary (Fortaleza, Brazil). Polyethylene (PE), polyethylene-polypropylene copolymer (PE-PP), polypropylene (PP), polystyrene (PS), polyethylene terephthalate (PET), and polyvinyl chloride (PVC).

decreased during the ebb tide and increased during the flood tide in both seasons (rainy and dry seasons), showing a positive correlation with water level. The shapes and colors of MPs varied significantly throughout the tidal cycle. The composition of MPs indicated that possible anthropogenic sources include wastewater discharges, solid waste disposal, coating materials, fishing activities, and tire wear particles.

The baseline data presented in this study are essential for filling knowledge gaps regarding the transport of MPs in estuaries and provide important information on the level of MP pollution in a low-inflow estuary where few studies exist. Our results and previous studies highlight that the local estuarine hydrodynamics is crucial to establish an adequate MP sampling since concentrations vary during a tidal cycle. Due to the lack of more intensive sampling, the results do not yet allow us to identify patterns for the estuary as a whole. To better understand the effects of tides on the transport of MPs in the estuary, we recommend investigating the variations along the estuary through more intensive spatial (longitudinal, transverse and vertical) and temporal sampling, as it is known that the abundance of MPs can vary depending on these variables (Li et al., 2023; Wong et al., 2020; Wu et al., 2022). Further research is needed to assess the role of other hydrodynamic factors in MP dynamics.

CRediT authorship contribution statement

Ravena Santiago Alves: Writing – review & editing, Writing – original draft, Visualization, Methodology, Investigation, Formal analysis, Data curation, Conceptualization. **Victória Maria Carneiro dos Santos:** Writing – original draft, Methodology, Investigation, Formal analysis. **Rebeca Amon Moreira:** Writing – original draft, Methodology, Investigation, Formal analysis. **Gabriel Chrystian Lima de Alcantara:** Writing – original draft, Methodology, Investigation, Formal analysis. **Emanuelle Ribeiro Lima:** Writing – original draft, Methodology, Investigation, Formal analysis. **Bárbara Pereira Paiva:** Visualization, Methodology, Formal analysis, Data curation. **Carlos Eduardo Peres Teixeira:** Writing – original draft, Visualization, Methodology, Conceptualization. **Vasco Stascxak Neto:** Writing – original draft, Methodology, Formal analysis. **Alejandro Pedro Ayala:** Writing – review & editing, Methodology, Formal analysis. **David Chelazzi:** Writing – original draft, Methodology, Formal analysis. **Johnny Peter Macedo Feitosa:** Writing – original draft, Methodology, Formal analysis. **Marcelo Oliveira Soares:** Writing – review & editing, Visualization, Supervision, Resources, Project administration, Methodology, Funding acquisition, Conceptualization. **Tommaso Giarrizzo:** Writing – review

& editing, Writing – original draft, Visualization, Supervision, Software, Methodology, Conceptualization. **Michael Barbosa Viana:** Writing – review & editing, Visualization, Supervision, Methodology, Conceptualization.

Declaration of competing interest

The authors declare that they have no known competing financial interests or personal relationships that could have appeared to influence the work reported in this paper.

Acknowledgements

This study is part of the project “I-Plastic: Dispersion and impacts of micro- and nano-plastics in the tropical and temperate oceans: from regional land-ocean interface to open ocean”. The authors would like to acknowledge the funding from the JPI Oceans International Consortium, INCT TMC Ocean, PROAP/CAPES and FUNCAP (Fundação Cearense de Apoio ao Desenvolvimento Científico e Tecnológico) for research activities. We thank the Conselho Nacional de Desenvolvimento Científico e Tecnológico for Research Productivity Fellowship (No. 313518/2020-3 and 315289/2021-0) PELD Costa Semiárida do Brasil-CSB (No. 442337/2020-5), CAPES-PRINT, CAPES-COFECUB, INCT TMC Ocean (405.765/2022-3), and Fundação Cearense de Apoio ao Desenvolvimento Científico e Tecnológico (Chief Scientist Program, PELD and and Pronen PNE-0112-00007.01.00/16) for their financial support. TG is funded by the Brazilian National Council for Scientific and Technological Development, CNPq (#308528/2022-0) and FUNCAP (UNI-0210-00136.01.00/23).

Appendix A. Supplementary data

Supplementary data to this article can be found online at <https://doi.org/10.1016/j.marpolbul.2024.117471>.

Data availability

Data available on request from the authors.

References

- Acharya, Sanjit, et al., 2021. Microfibers from synthetic textiles as a major source of microplastics in the environment: a review. *Text. Res. J.* 91 (17–18), 2136–2156. <https://doi.org/10.1177/0040517521991244>.
- Anderson, T., 2008. *The Theory and Practice of Online Learning*. Athabasca University Press, Athabasca.
- Banik, Partho, et al., 2024. Quantification, characterization and risk assessment of microplastics from five major estuaries along the northern Bay of Bengal coast. *Environ. Pollut.* 342, 123036. <https://doi.org/10.1016/j.envpol.2023.123036>.
- Biltcliff-Ward, Adam, et al., 2022. The estuarine plastics budget: a conceptual model and meta-analysis of microplastic abundance in estuarine systems. *Estuar. Coast. Shelf Sci.* 275, 107963. <https://doi.org/10.1016/j.ecss.2022.107963>.
- Cardoso-Mohedano, Jose Gilberto, et al., 2023. Microplastics transport in a low-inflow estuary at the entrance of the Gulf of California. *Sci. Total Environ.* 870, 161825. <https://doi.org/10.1016/j.scitotenv.2023.161825>.
- Chinfak, Narainrit, et al., 2021. Abundance, composition, and fate of microplastics in water, sediment, and shellfish in the Tapi-Phumduang River system and Bandon Bay, Thailand. *Sci. Total Environ.* 781, 146700. <https://doi.org/10.1016/j.scitotenv.2021.146700>.
- Clarke, K.R., Gorley, R.N., 2015. *PRIMER v7: User Manual/Tutorial*. PRIMER-E Plymouth.
- Cohen, Jonathan H., et al., 2019. Observations and simulations of microplastic debris in a tide, wind, and freshwater-driven estuarine environment: the Delaware Bay. *Environ. Sci. Technol.* 53 (24), 14204–14211. <https://doi.org/10.1021/acs.est.9b04814>.
- Cunningham, Brittany, et al., 2022. Toxicity of micro and nano tire particles and leachate for model freshwater organisms. *J. Hazard. Mater.* 429, 128319. <https://doi.org/10.1016/j.jhazmat.2022.128319>.
- De Frond, Hannah, et al., 2021. μ ATR-FTIR spectral libraries of plastic particles (FLOPP and FLOPP-e) for the analysis of microplastics. *Anal. Chem.* 93 (48), 15878–15885. <https://doi.org/10.1021/acs.analchem.1c02549>.
- Defontaine, Sophie, Jalón-Rojas, Isabel, 2023. Physical processes matters! Recommendations for sampling microplastics in estuarine waters based on

- hydrodynamics. *Mar. Pollut. Bull.* 191, 114932. <https://doi.org/10.1016/j.marpolbul.2023.114932>.
- Devereux, Ria, et al., 2023. "The great source" microplastic abundance and characteristics along the river Thames. *Mar. Pollut. Bull.* 191, 114965. <https://doi.org/10.1016/j.marpolbul.2023.114965>.
- Diansyah, Gusti, et al., 2024. Dynamics of microplastic abundance under tidal fluctuation in Musi estuary, Indonesia. *Mar. Pollut. Bull.* 203, 116431. <https://doi.org/10.1016/j.marpolbul.2024.116431>.
- Díez-Pérez, Diana Beatriz, et al., 2023. Microplastics in surface water of the Bay of Asunción, Paraguay. *Mar. Pollut. Bull.* 192, 115075. <https://doi.org/10.1016/j.marpolbul.2023.115075>.
- Elizalde-Velázquez, Gustavo Axel, Gómez-Oliván, Leobardo Manuel, 2021. Microplastics in aquatic environments: a review on occurrence, distribution, toxic effects, and implications for human health. *Sci. Total Environ.* 780, 146551. <https://doi.org/10.1016/j.scitotenv.2021.146551>.
- Freedman, David, Lane, David, 1983. A nonstochastic interpretation of reported significance levels. *J. Bus. Econ. Stat.* 1 (4), 292–298. <https://doi.org/10.2307/1391660>.
- Freitas, Pedro Paulo, Menezes, Maria Ozileia Bezerra, Schettini, Carlos Augusto França, 2016. Hydrodynamics and particulate suspended matter transport in a shallow and highly urbanized estuary: the Cocó estuary, Fortaleza, Brazil. *Brazilian J. Geophys.* 33 (4), 579–590. <https://doi.org/10.22564/rbgf.v33i4.754>.
- Gago, J., et al., 2018. Standardised Protocol for Monitoring Microplastics in Seawater. JPI-Oceans BASEMAN project. <https://doi.org/10.13140/RG.2.2.14181.45282>.
- Giarratano, Erica, et al., 2022. The Chubut River estuary as a source of microplastics and other anthropogenic particles into the Southwestern Atlantic Ocean. *Mar. Pollut. Bull.* 185, 114267. <https://doi.org/10.1016/j.marpolbul.2022.114267>.
- Govender, Joeline, et al., 2020. Towards characterising microplastic abundance, typology and retention in mangrove-dominated estuaries. *Water* 12 (10), 2802. <https://doi.org/10.3390/w12102802>.
- Han, M., et al., 2020. Distribution of microplastics in surface water of the lower Yellow River near estuary. *Sci. Total Environ.* 707, 135601. <https://doi.org/10.1016/j.scitotenv.2019.135601>.
- Harris, Peter T., 2020. The fate of microplastic in marine sedimentary environments: a review and synthesis. *Mar. Pollut. Bull.* 158, 111398. <https://doi.org/10.1016/j.marpolbul.2020.111398>.
- He, Pinjing, et al., 2019. Municipal solid waste (MSW) landfill: a source of microplastics?—evidence of microplastics in landfill leachate. *Water Res.* 159, 38–45. <https://doi.org/10.1016/j.watres.2019.04.060>.
- Hidalgo-Ruz, Valeria, et al., 2012. Microplastics in the marine environment: a review of the methods used for identification and quantification. *Environ. Sci. Technol.* 46 (6), 3060–3075. <https://doi.org/10.1021/es2031505>.
- Hossain, M. Belal, et al., 2023. Microplastics in surface water from a mighty subtropical estuary: first observations on occurrence, characterization, and contamination assessment. *Environ. Res.* 226, 115594. <https://doi.org/10.1016/j.envres.2023.115594>.
- INMET, et al., 2020. <https://clima.inmet.gov.br/GraficosClimatologicos/CE/82397>. (Accessed 12 March 2024).
- Jayalakshamma, Meghana Parameswarappa, et al., 2023. Characterizing microplastics in urban runoff: a multi-land use assessment with a focus on 1–125 µm size particles. *Sci. Total Environ.* 904, 166685. <https://doi.org/10.1016/j.scitotenv.2023.166685>.
- Jin, Naifu, et al., 2022. Characterization and identification of microplastics using Raman spectroscopy coupled with multivariate analysis. *Anal. Chim. Acta* 1197, 339519. <https://doi.org/10.1016/j.aca.2022.339519>.
- Kole, Pieter Jan, et al., 2017. Wear and tear of tyres: a stealthy source of microplastics in the environment. *Int. J. Environ. Res. Public Health* 14 (10), 1265. <https://doi.org/10.3390/ijerph14101265>.
- Kroon, Frederieke, et al., 2018. A workflow for improving estimates of microplastic contamination in marine waters: a case study from North-Western Australia. *Environ. Pollut.* 238, 26–38. <https://doi.org/10.1016/j.envpol.2018.03.010>.
- Lam, Theresa Wing Ling, et al., 2020. Spatial variation of floatable plastic debris and microplastics in the Pearl River Estuary, South China. *Mar. Pollut. Bull.* 158, 111383. <https://doi.org/10.1016/j.marpolbul.2020.111383>.
- Largier, John L., 2023. Recognizing low-inflow estuaries as a common estuary paradigm. *Estuar. Coasts* 46 (8), 1949–1970. <https://doi.org/10.1007/s12237-023-01271-1>.
- Leads, Rachel R., Weinstein, John E., 2019. Occurrence of tire wear particles and other microplastics within the tributaries of the Charleston Harbor Estuary, South Carolina, USA. *Mar. Pollut. Bull.* 145, 569–582. <https://doi.org/10.1016/j.marpolbul.2019.06.061>.
- Li, B., et al., 2023. Dynamic characteristics of microplastics under tidal influence and potential indirect monitoring methods. *Sci. Total Environ.* 869, 161869. <https://doi.org/10.1016/j.scitotenv.2023.161869>.
- Lima, A.R.A., et al., 2015. Seasonal distribution and interactions between plankton and microplastics in a tropical estuary. *Estuar. Coast. Shelf Sci.* 165, 213–225. <https://doi.org/10.1016/j.ecss.2015.05.018>.
- Lin, Lang, et al., 2020. Low level of microplastic contamination in wild fish from an urban estuary. *Mar. Pollut. Bull.* 160, 111650. <https://doi.org/10.1016/j.marpolbul.2020.111650>.
- Liu, X., et al., 2022. Ecological interception effect of mangroves on microplastics. *J. Hazard. Mater.* 423, 127231. <https://doi.org/10.1016/j.jhazmat.2021.127231>.
- Malli, A., et al., 2022. Transport mechanisms and fate of microplastics in estuarine compartments: a review. *Mar. Pollut. Bull.* 177. <https://doi.org/10.1016/j.marpolbul.2022.113553>.
- Molisaní, Mauricio Mussi, et al., 2006. Estimativa da descarga fluvial para os estuários do Estado do Ceará, Brasil. *Arquivo de Ciências do Mar* 39, 53–60. <http://periodicos.ufc.br/arquivosdecienciadomar/article/view/6173>.
- Moura, Victor Lacerda, Lacerda, Luiz Drude, 2022. Mercury sources, emissions, distribution and bioavailability along an estuarine gradient under semiarid conditions in northeast Brazil. *Int. J. Environ. Res. Public Health* 19 (24), 17092. <https://doi.org/10.3390/ijerph192417092>.
- Munno, Keenan, et al., 2023. Patterns of microparticles in blank samples: a study to inform best practices for microplastic analysis. *Chemosphere* 333, 138883. <https://doi.org/10.1016/j.chemosphere.2023.138883>.
- Olivatto, Gláucia P., et al., 2019. Microplastic contamination in surface waters in Guanabara Bay, Rio de Janeiro, Brazil. *Mar. Pollut. Bull.* 139, 157–162. <https://doi.org/10.1016/j.marpolbul.2018.12.042>.
- Oo, Phyto Zaw, et al., 2021. Horizontal variation of microplastics with tidal fluctuation in the Chao Phraya River Estuary, Thailand. *Mar. Pollut. Bull.* 173, 112933. <https://doi.org/10.1016/j.marpolbul.2021.112933>.
- Osman, Ahmed I., et al., 2023. Microplastic sources, formation, toxicity and remediation: a review. *Environ. Chem. Lett.* 21 (4), 2129–2169. <https://doi.org/10.1007/s10311-023-01593-3>.
- Pasquier, Gabriel, et al., 2024. Do tidal fluctuations affect microplastics distribution and composition in coastal waters? *Mar. Pollut. Bull.* 200, 116166. <https://doi.org/10.1016/j.marpolbul.2024.116166>.
- Pereira, S.P., et al., 2015. Modeling of coastal water contamination in Fortaleza (Northeastern Brazil). *Water Sci. Technol.* 72 (6), 928–936. <https://doi.org/10.2166/wst.2015.292>.
- Prabakaran, R., et al., 2002. Structural investigation of copper phthalocyanine thin films using X-ray diffraction, Raman scattering and optical absorption measurements. *Phys. Status Solidi B* 229 (3), 1175–1186. [https://doi.org/10.1002/1521-3951\(200202\)229:3<1175::AID-PSSB1175>3.0.CO;2-K](https://doi.org/10.1002/1521-3951(200202)229:3<1175::AID-PSSB1175>3.0.CO;2-K).
- Praved, P. Hari, et al., 2024. Evaluation of microplastic pollution and risk assessment in a tropical monsoonal estuary, with special emphasis on contamination in jellyfish. *Environ. Pollut.* 123158. <https://doi.org/10.1016/j.envpol.2023.123158>.
- Rajan, Kumar, et al., 2023. Spatio-temporal patterns of microplastic contamination in surface waters of Hooghly River Estuary: causes and consequences. *Reg. Stud. Mar. Sci.* 65, 103111. <https://doi.org/10.1016/j.rsma.2023.103111>.
- Ren, Lihui, et al., 2023. Identification of microplastics using a convolutional neural network based on micro-Raman spectroscopy. *Talanta* 260, 124611. <https://doi.org/10.1016/j.talanta.2023.124611>.
- SEMACE, 2010. Parque Ecológico do Rio Cocó. <https://www.semace.ce.gov.br/2010/12/08/paquer-ecologico-do-rio-coco/>. (Accessed 12 March 2024).
- SNIS, 2022. Painel Saneamento Brasil: Município Fortaleza. <https://www.painelsaneamento.org.br/localidade?id=230440>. (Accessed 20 July 2024).
- Soares, M.O., et al., 2021. Challenges and perspectives for the Brazilian semi-arid coast under global environmental changes. *Perspectives in Ecology and Conservation* 19 (3), 267–278. <https://doi.org/10.1016/j.pecon.2021.06.001>.
- Sorasan, Carmen, et al., 2022. Ageing and fragmentation of marine microplastics. *Sci. Total Environ.* 827, 154438. <https://doi.org/10.1016/j.scitotenv.2022.154438>.
- Stead, J.L., et al., 2020. Identification of tidal trapping of microplastics in a temperate salt marsh system using sea surface microlayer sampling. *Sci. Rep.* 10 (1). <https://doi.org/10.1038/s41598-020-70306-5>.
- Sukhsangchan, Roachira, et al., 2020. Suspended microplastics during a tidal cycle in sea-surface waters around Chao Phraya River mouth, Thailand. *ScienceAsia* 46 (6), 724. <https://www.thaiscience.info/Journals/Article/SCAS/10992774.pdf>.
- Tang-Siri, Jiradet, et al., 2024. Occurrence of microplastics and ecological risk assessment during tidal changes in the Chao Phraya River estuary, Thailand. *Mar. Environ. Res.* 200, 106647. <https://doi.org/10.1016/j.marenvres.2024.106647>.
- Tangsongcharoen, W., Paulis, M., 2024. Effect of plasticizer release on the final properties of blend, hybrid and block copolymer latex films containing hard and soft phases. *Prog. Org. Coat.* 196, 108730. <https://doi.org/10.1016/j.porgcoat.2024.108730>.
- Vasconcelos, Francisca Dalila Menezes, et al., 2021. Quality index of permanent preservation areas of urban water resources: PPAWater. *Revista Ambiente & Água* 16 (1), e2589. <https://doi.org/10.4136/ambi-agua.2589>.
- Wang, Teng, et al., 2019. Preliminary study of the source apportionment and diversity of microplastics: taking floating microplastics in the South China Sea as an example. *Environ. Pollut.* 245, 965–974. <https://doi.org/10.1016/j.envpol.2018.10.110>.
- Ward, Raymond D., et al., 2023. Vertical accretion rates of mangroves in northeast Brazil: implications for future responses and management. *Estuar. Coast. Shelf Sci.* 289, 108382. <https://doi.org/10.1016/j.ecss.2023.108382>.
- Watkins, Lisa, et al., 2021. What you net depends on if you grab: a meta-analysis of sampling method's impact on measured aquatic microplastic concentration. *Environ. Sci. Technol.* 55 (19), 12930–12942. <https://doi.org/10.1021/acs.est.1c03019>.
- Wei, N., et al., 2023. Dynamic signatures of microplastic distribution across the water column of Yangtze River Estuary: complicated implication of tidal effects. *Mar. Environ. Res.* 106005. <https://doi.org/10.1016/j.marenvres.2023.106005>.
- Wong, Graham, et al., 2020. Microplastic pollution of the Tamsui River and its tributaries in northern Taiwan: spatial heterogeneity and correlation with precipitation. *Environ. Pollut.* 260, 113935. <https://doi.org/10.1016/j.envpol.2020.113935>.
- Wright, Stephanie L., et al., 2013. The physical impacts of microplastics on marine organisms: a review. *Environ. Pollut.* 178, 483–492. <https://doi.org/10.1016/j.envpol.2013.02.031>.
- Wu, Y., et al., 2022. Vertical distribution and river-sea transport of microplastics with tidal fluctuation in a subtropical estuary, China. *Sci. Total Environ.* 822. <https://doi.org/10.1016/j.scitotenv.2022.153603>.
- Wu, Panfeng, et al., 2024. Seasonal dynamics, tidal influences, and anthropogenic impacts on microplastic distribution in the Yangtze River Estuary: a comprehensive characterization and comparative analysis. *J. Hazard. Mater.* 135167. <https://doi.org/10.1016/j.jhazmat.2024.135167>.

Xu, Jun-Li, et al., 2019. FTIR and Raman imaging for microplastics analysis: state of the art, challenges and prospects. *TrAC Trend. Anal. Chem.* 119, 115629. <https://doi.org/10.1016/j.trac.2019.115629>.

Zhang, Jiaxu, et al., 2019. Microplastics in the surface water of small-scale estuaries in Shanghai. *Mar. Pollut. Bull.* 149, 110569. <https://doi.org/10.1016/j.marpolbul.2019.110569>.

Zheng, Y., et al., 2021. Comparative study of three sampling methods for microplastics analysis in seawater. *Sci. Total Environ.* 765, 144495. <https://doi.org/10.1016/j.scitotenv.2020.144495>.